Experimental and Numerical Investigation of the Turbulent Flow behind a Backward-Facing Step

Tatiana G. ELIZAROVA[1], Eugene V. SHILNIKOV[1],
Régine WEBER[2], Jacques HUREAU[2], Jean-Claude LENGRAND[3]

[1] Inst. for Math. Modelling, Russian Academy of Sciences,
Miusskaya Square, 4a, Moscow 125047, Russia, elizar@imamod.com
[2] Lab. de Mécanique et d'Energétique, Polytech'Orléans,
8, Rue Léonard de Vinci, 45072 Orléans Cedex 2, France, Regine.Weber@univ-orleans.fr
[3] Lab. d'Aérothermique du CNRS, 1C, Av. de la Rech. Scientifique,
45071 Orléans Cedex 2, France, lengrand@cnrs-orleans.fr

1. Introduction

The problem considered in the present study is the flow behind a backward facing step. Experiments were performed at LME in a wind tunnel adapted for low velocities. Particle Image Velocimetry (PIV) was used to measure the mean velocity field behind the step.

Numerical calculations were performed using the quasi-hydrodynamic (QHD) equations that differ from the Navier-Stokes (NS) ones by additional dissipative terms. These terms include a multiplying factor τ, which has the dimension of a time. For laminar flows, τ is related to the molecular viscosity coefficient. For turbulent flows the value of τ is no longer related with molecular viscosity and must be adjusted to fit the general flow features. The general form of QHD equations can be found in, e.g. [1], [2].

For small Reynolds numbers corresponding to the laminar regime, numerical calculations show that the flow is stationary. The numerical flow structure is in good agreement with the solution of NS numerical modelling and known experimental results [3].

For larger Reynolds numbers, corresponding to the turbulent regime, the calculated flow becomes strongly non-stationary and depends on the additional viscosity level (i.e. on the value of τ). By varying τ, it is possible to find a flow structure that corresponds to the wind tunnel experiments.

The geometry of the flow studied in this paper is shown in Figure 1. The Reynolds number Re is calculated as Vh/ν, where V is the average speed of the flow at the channel entrance section, h the step height, and ν the kinematic viscosity coefficient. Experiments were performed to determine the mean velocity field behind the step and then the length of the recirculation area.

The first computational and experimental results were presented in [3].

2. Experimental setup

2..1. Wind tunnel

The experimental results have been obtained in an open air-driven wind tunnel at LME (Orléans, France). The existing square section (300×300 mm) has been adapted to present a two-dimensional backward-facing step with adjustable step height. The width and the length (800 mm) of the test section were not modified. The electrically powered fan allows us to obtain velocities of about 1 to 80 m/s in the non-adapted test section without any obstacle. Previous works published in the literature about this subject [4] pointed out that the reattachment length L of the flow behind the step varies with the Re number and the height h of the step: L can be twenty times larger than h. So, to be able to visualize the whole flowfield (and especially the reattachment area), the test section height H' upstream of the step is fixed to 51 mm and

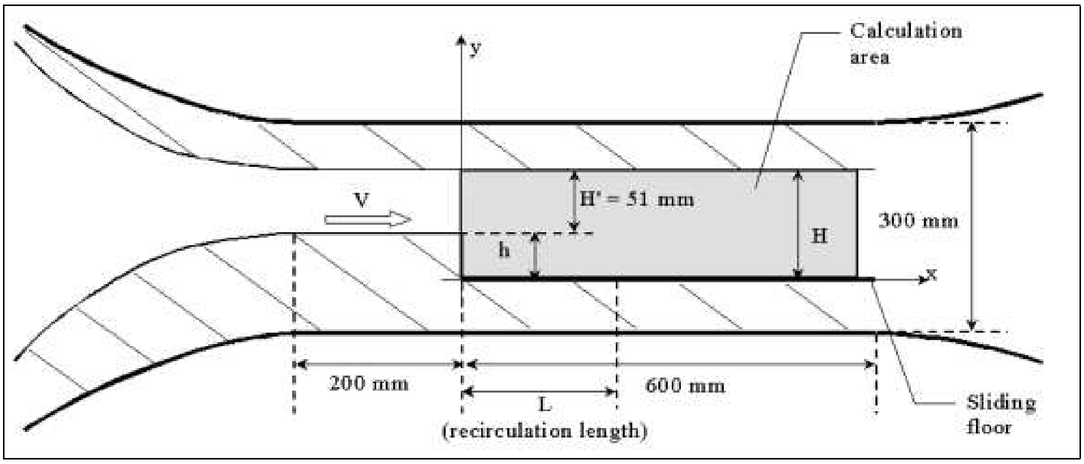

Figure 1: Wind tunnel section and notations.

we have considered different step heights between 12 mm and 50 mm. The length of the test section before the step is 200 mm to allow the flow to be fully developed. The mean velocity obtained is approximately 1.4 m/s. Preliminary measurements with a two-components hot-wire anemometer allowed us to verify that this velocity is stable and uniform. The mean turbulent ratio then measured is less than 0.85 % ahead of the step. One wall is transparent, for direct visualization, and the other ones are black. A laser sheet enters the wind tunnel section through a glass window in the upper wall.

2..2. Particule Image Velocimetry (PIV)

The experimental data generated are the two-dimensional components of the velocity behind the backward-facing step. In our case, an oil generator, placed at the entrance of the tranquillization room (velocity about 0.01 m/s), is used to generate and supply tracer particles. The mean diameter of the particles is about 1 μm. The laser sheet is generated by a double-oscillator laser: a Nd/Yag laser (Spectra Physics 400) adjusted on the second harmonic and emitting two pulses of 200 mJ each ($\lambda = 532$ nm), at a repetition rate of 10 Hz. The laser sheet is developed with an optical arm containing mirrors. Lenses allowed us to obtain a laser sheet with a divergence of about 60° and with a thickness of about 1 mm around the step. For the present experimental data, the flow images are picked up by a PIVCAM CCD camera with 1008 $\times$ 1016 sensor elements, placed perpendicularly to the laser sheet. The laser pulses are synchronized with the image acquisition by a TSI synchronizer system driven by the InSight-NT^{TM} software. As stated previously, the reattachment length can be as long as twenty times the height of the step. The aim of these experimental measurements is to obtain the mean flow behind the step, so we have chosen to decompose the flow area into several visualized areas (80×80 mm or 135×135 mm) to ensure a good precision in the wake of the step. This is only possible because the mean velocity field is studied. These sub-areas overlap by about 10 mm. For all the results presented here, the PIV recordings are divided into interrogation areas corresponding to 64 $\times$ 64 pixels. For data post-processing, the interrogation areas overlap by 50%. The local displacement vector is determined for each interrogation area by statistical methods (auto-correlation). The projection of the local flow velocity vector onto the laser sheet plane is calculated by InSight using the time delay between the two illuminations ($\Delta t = 1$ ms) and the magnification at imaging. The post-processing used here is very simple – no more than a velocity range filter.

3. Numerical approach

The gas in the wind-tunnel is air taken at room temperature and atmospheric pressure. The entrance velocity is $U_0 = 1.2 - 1.4$ m/s. The speed of sound in air under normal conditions equals

$c_s = 340\,\mathrm{m/s}$. Therefore, the Mach number is small ($U_0/c_s \sim 0.003$), which allows us to apply the approximation of viscous incompressible isothermal liquid. In the experiment visualization is done in the symmetry plane of the device; therefore, a flat two-dimensional model of the flow is used for numerical computations.

Quasi-hydrodynamic (QHD) equations for the incompressible viscous flows in the absence of the external forces can be written in the index form as, e.g. [1], [5], [3].

$$\nabla_i u^i = \nabla_i w^i, \tag{1}$$

$$\frac{\partial u^k}{\partial t} + \nabla_i(u^i u^k) + \frac{1}{\rho}\nabla^k p = \nabla_i\ \Pi^{ik}_{NS} + \nabla_i(u^i w^k) + \nabla_i(w^i u^k), \tag{2}$$

$$\frac{\partial T}{\partial t} + \nabla_i(u^i T) = \nabla_i(w^i T) + \kappa \nabla_i T, \tag{3}$$

where the Navier-Stokes viscous stress tensor is

$$\Pi^{ik}_{NS} = \nu(\nabla^k u^i + \nabla^i u^k) \tag{4}$$

and vector w is defined as

$$\tau(u^j \nabla_j u^k + \frac{1}{\rho}\nabla^k p). \tag{5}$$

In equations (1) - (5) $\rho = \mathrm{const}$ is the density, ν is the kinematic viscosity, κ is the thermal conductivity, τ is an adjustable characteristic time. In the limit $\tau \to 0$ QHD system reduces to the classical Navier-Stokes equations.

We considered a plane two-dimensional isothermal flow in a channel of height $H' + h$. For the numerical integration of the QHD equations we implemented an explicit finite-volume algorithm of the second order space accuracy as described in [5].

4. Results for Re=4667 and Re=4012

The experimental (Figs. 3, 5) and numerical (Figs. 2, 4) flow patterns (stream functions) for $Re = 4667$ are shown below. The experimental ones are obtained by PIV technique. In QHD calculations, τ was set to 3.6×10^{-3}s.

Fig. 3 shows the time sequence of experimental flowfields obtained at a frequency of 10 Hz in a part of the flow domain behind the step. The field of velocity vectors is obtained by inter-correlation between two images acquired with a time interval of 1 ms (instantaneous flowfields). The flow presents a non-stationary character. Fig. 5 shows the whole flowfield averaged over a time interval of approximately 10 s. For this time interval the flowfield looks stationary.

Each numerical pattern shown in Fig. 2 is constructed from the instantaneous velocity vectors averaged over the same time intervals as the instantaneous experimental ones (actually averaged over 0.001 s) and for the same part of the flow domain. The numerical flowfields are obtained at a time interval $\sim$ 0.1 s. (to reproduce the experimental acquisition frequency of frequency $\sim$ 10 Hz). Fig. 2 exhibits the same chaotic and unsteady character as the experiment (Fig. 3). When averaged over more than approximately 2 s, the numerical flowfield appears to be nearly stationary (Fig. 4) and in good agreement with the corresponding experimental one (Fig. 5).

Similar numerical (with $\tau = 3.2 \times 10^{-3}$ s) and experimental results for Re = 4012, are shown in Figs. 6 - 9. A sequence of 8 "instantaneous" numerical and experimental flowfields are presented in Figs. 6 and 7. In Fig. 8 three numerical flowfields averaged over slightly different time intervals exhibit nearly identical flow patterns as three averaged experimental ones (Fig. 9).

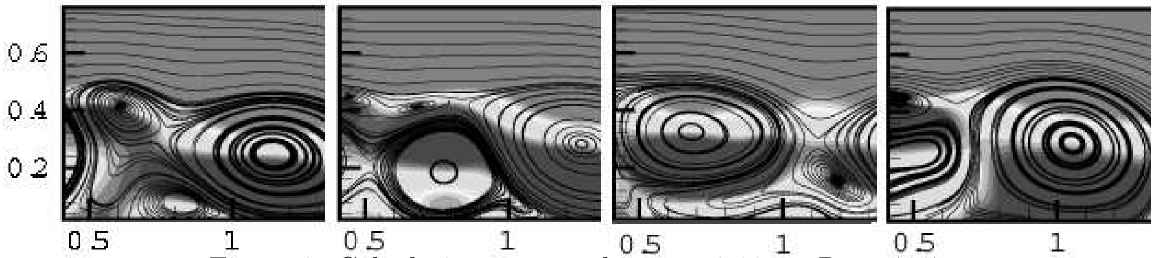

Figure 2: Calculation, averaged over $\sim 0.001\,\mathrm{s}$, $Re = 4667$

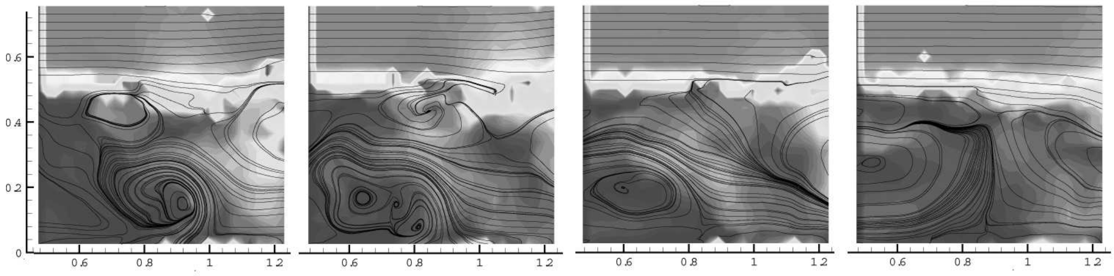

Figure 3: Experiment, averaged over $\sim 0.001\,\mathrm{s}$, $Re = 4667$

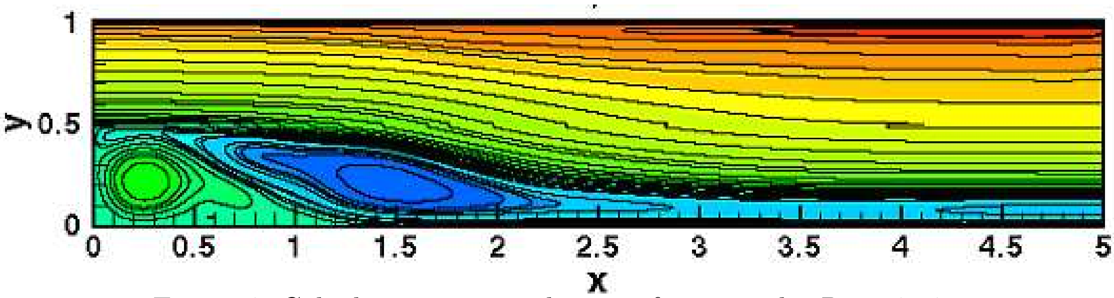

Figure 4: Calculation, averaged over a few seconds, $Re = 4667$

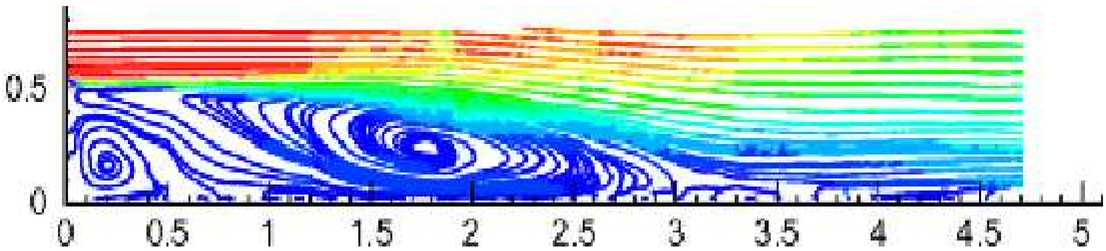

Figure 5: Experiment, averaged over a few seconds, $Re = 4667$

5. Discussion and conclusions

The time resolution of numerical results was much smaller than the experimental one. That is why the comparison between numerical and experimental results was done on average velocities, with an averaging time ranging from 1 ms to a few seconds.

The features of the averaged flow depends both on the value of the temporal smoothing parameter τ (which makes the difference between the QHD system and the Navier-Stokes equations) and on the averaging interval.

In spite of considerable simplifications of the problem - two-dimensional model of a viscous non-compressible isothermal flow - the computational results are in good agreement with the experimental ones.

We suppose that the numerical modelling of the turbulent flow behind the step by means of the QHD system is possible due to the additional (compared with the Navier-Stokes equations) dissipative terms that are small for stationary flows and become not small for non-stationary turbulent flows.

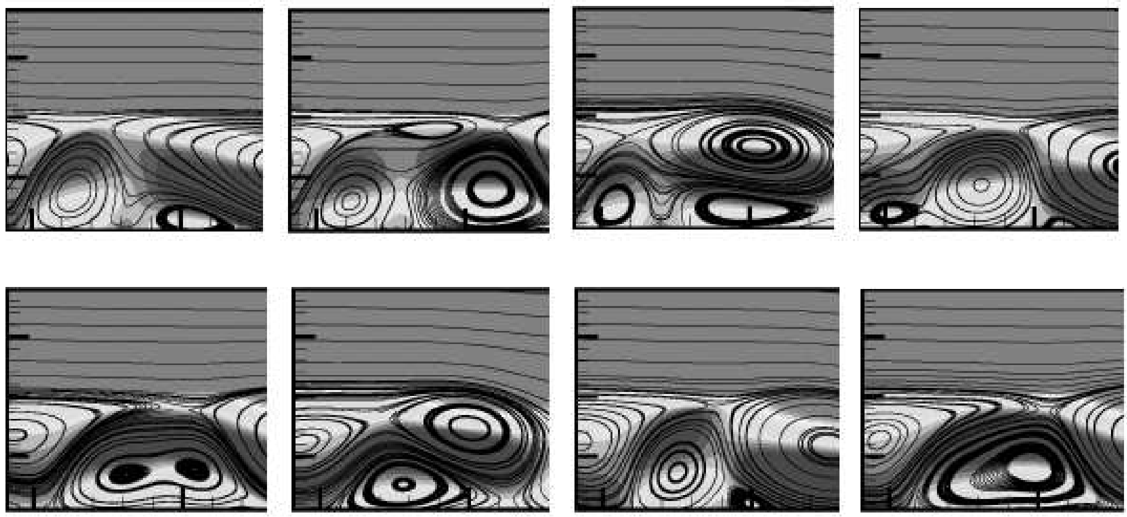

Figure 6: Calculation, averaged over $\sim 0.001\,\mathrm{s}$, $Re = 4012$

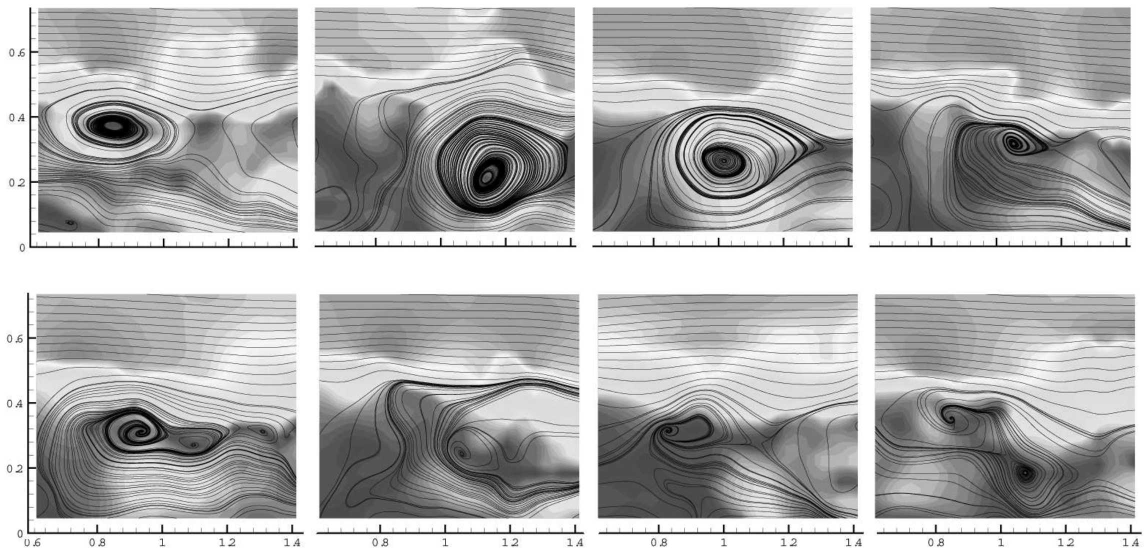

Figure 7: Experiment, averaged over $\sim 0.001\,\mathrm{s}$, $Re = 4012$

References

[1] T.G. Elizarova and Yu.V. Sheretov, “Theoretical and numerical investigation of quasi-gasdynamic and quasi-hydrodynamic equations”, *J. Comput. Mathem. and Mathem. Phys.*, **41** 219–234 (2001).

[2] T.G. Elizarova and Yu.V. Sheretov , “Analyse du problème de l’écoulement gazeux dans les microcanaux par les équations quasi hydrodynamiques”, *La Houille Blanche*, **5**, 66–72 (2003).

[3] T.G. Elizarova, I.S. Kalachinskaya, R. Weber, J. Hureau and J.-C. Lengrand, “Ecoulement derriere une marche. Etude expérimentale et numérique”, *Laboratoire d’Aérothermique du CNRS/Orléans (France)*, rapport R 2001–1 (2001).

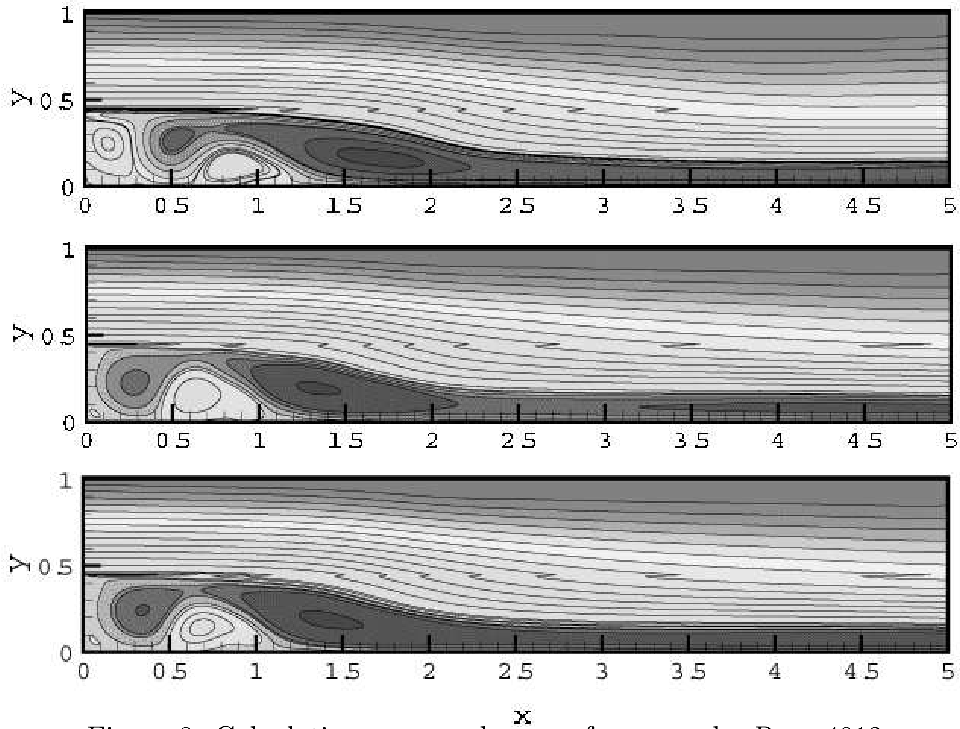

Figure 8: Calculation, averaged over a few seconds, $Re = 4012$

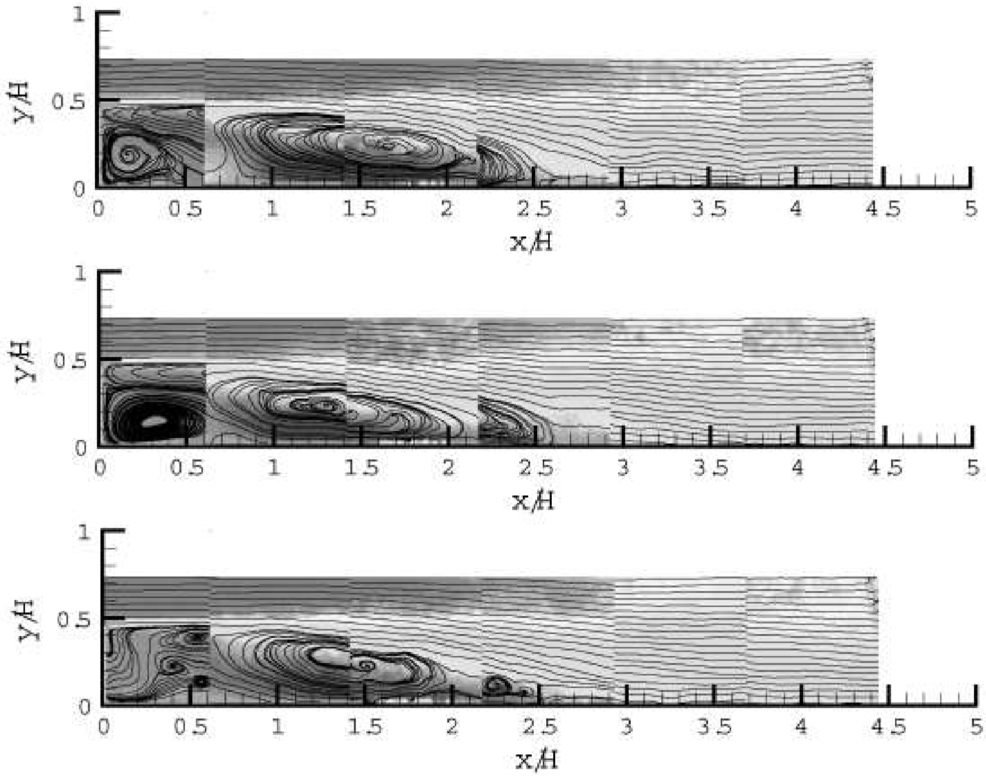

Figure 9: Experiment, averaged over a few seconds, $Re = 4012$

[4] B.F. Armaly, F. Durst, J.C.F. Pereira, B. Schonung, "Experimental and theoretical investigation of backward-facing step flow", *J. Fluid Mech.*, **127** 473–496 (1983).

[5] T.G. Elizarova and O.Yu. Milyukova, "Numerical Simulation of Viscous Incompressible Flow in a Cubic Cavity", *J. Comp.Mathem. and Math. Phys.*, **43** 453–466 (2003).